FLUORESCENT MOLECULAR ROTORS AS PROBES FOR POLYMERS

Marie-Christiane Carré [1], Catherine Dorion [1], Richard Rebizak [1], Fernand Pla [2], Alain Brembilla [3], Marie-Laure Viriot [1] *

[1] Département de Chimie Physique des Réactions (GRAPP) - URA 328 CNRS,
[2] Laboratoire des Sciences du Génie Chimique (GRC) - UPR 6811 CNRS and
[3] Laboratoire de Chimie Physique Macromoléculaire - URA 494 CNRS,
ENSIC-INPL, 1, rue Grandville BP 451 F-54001 Nancy Cedex - France

ABSTRACT

The use of a molecular rotor (1,1-dicyano-4-(4'-dimethylaminophenyl)-1,3-butadiene) as a fluorescent probe was proved to be of great interest for the study of polymers. First, the rotor can detect the critical time of the glass effect in the bulk polymerization of MMA into PMMA due to viscosity change, this will allow a better control of the process and is complementary to the information issued from the use of the fluorescent pyrene probe which is sensitive to the gel effect. Second, the cinnamylidene rotor was able to detect the formation of hydrophobic microdomains for cationic amphiphilic polymers in their aggregation modes when they were solubilized in water, both polarity and viscosity changes are playing a role. The possibility of incorporation of various molecular fluorescent rotors in polymers beads was also studied.

ABBREVIATIONS

CTABr, cetyltrimethylammonium bromide ; HEPBr, 1-hexadecyl-3-ethylpyridinium bromide ; HMIBr, 1-methyl-3-hexadecylimidazolium bromide ; MMA, methylmethacrylate ; PMMA, poly(methylmethacrylate) ; PVIC1Br, poly(1-methylvinylimidazolium bromide) ; PVIC16Br, poly(1-hexadecylvinylimidazolium bromide) ; P3VPC1Br, poly(1-methyl-3-vinylpyridinium bromide) ; P3VPC16Br, poly(1-hexadecyl-3-vinylpyridinium bromide).

INTRODUCTION

Molecular rotors, structure of which can be (4-dimethylamino)-benzene, -benzylidene or -cinnamylidene derivatives, have photophysical characteristics which strongly depend on the environmental parameters (polarity, viscosity, temperature, etc.).

 CCC 1022-1360/98/$ 10.00

Use of fluorescent molecular rotors as sensors in polymers will be described in three studies : (i) the detection of the glass effect in the bulk polymerization of MMA taking advantage of the viscosity change, (ii) the detection of hydrophobic microdomains in amphiphilic polymers due to the change in both the polarity and the viscosity when the aggregation is performed and (iii) the possible incorporation in polymer beads using emulsion polymerization.

Before to describe these studies, we will remain some basic knowledge on molecular fluorescent rotors. Moreover, as we have used the fluorescent pyrene probe for complementary studies or to run comparison in the use of the two types of fluorescent tracers, we will also briefly recall the characteristics of pyrene fluorescence.

Molecular rotors of the type benzylidene or cinnamylidene (as an example, 1,1-dicyano-(4'-dimethylaminophenyl)-1,3-butadiene, whose structure and schematic photophysical behavior are indicated in Fig. 1) can be used as polarity and/or viscosity fluorescent probes, because their fluorescence emission wavelength at their maximum, $\lambda_{f\,max}$, is dependent on the *polarity* of the medium (an increase of the polarity enhances the stability of the charge transfer excited state) and their fluorescence efficiency expressed as the fluorescence quantum yield is dependent on the *viscosity* of the medium (an increase of the local viscosity involves a diminution of the medium free volume with a slowing down of the intramolecular rotor motion and then a reduction of the non radiative deactivation processes) (Refs. 1-3).

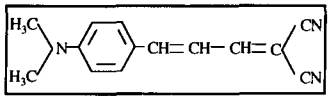

Rotor $\xrightarrow{I_{ab}}$ Rotor * *Photonic absorption*

Rotor * $\xrightarrow{k_r}$ Rotor + $h\nu_f$ *Fluorescence emission*

Rotor * $\xrightarrow{k_{nr}}$ Rotor *Non radiative processes*

Fig. 1 : Molecular structure of the fluorescent rotor and photophysical processes.

For a molecular rotor, the fluorescence quantum yield is expressed by the eq. 1 (Ref. 1), where k_r and k_{nr} represent respectively the rates of radiative and non radiative deactivation processes :

$$\Phi_f = \frac{k_r}{k_r + k_{nr}} \qquad \text{(eq. 1)}$$

Note that the fluorescence intensity is directly related to the fluorescence quantum yield if the light absorbed intensity is known ($I_f = \Phi_f I_{ab}$).

Several authors have also shown that taking into account the free volume theory (Refs. 1, 4), it becomes possible to express the fluorescence quantum yield through the eq. 2, where k_{nr}^0 is the rate constant of the rotor at the free state, b is a characteristic constant of the molecular rotor, and v_0 and v_f are respectively the volume of the rotor and the free volume of the solvent :

$$\Phi_f \approx \frac{k_r}{k_{nr}^0} \exp \frac{bv_0}{v_f} \qquad \text{(eq. 2)}$$

If the relation between the solvent viscosity and the free volume (Ref. 5) is considered, the fluorescence quantum yield can be expressed also by the eq. 3, where B is a constant, T the temperature and x a value depending of the medium :

$$\Phi_f = B \left(\frac{\eta}{T} \right)^x \qquad \text{(eq. 3)}$$

Pyrene represents a well known fluorescent probe, as (i) a *polarity probe* because of the vibronic structure dependence of the fluorescence monomer on the polarity of the medium expressed as the ratio I_1/I_3, where I_1 and I_3 are respectively the emission bands 1 and 3 (the ratio I_1/I_3 increases with an enhancement of the polarity) (Ref. 6) as well as (ii) a *viscosity probe* because of the dependence of the rate constant k_d for the intermolecular formation of the excimer on the lateral diffusion in the medium (an increase of the viscosity limits the diffusion of ground state pyrene molecules towards the excited state Py * ones (Fig. 2) and lowers the rate k_d). The ratio I_{ex}/I_{mon}, which can be expressed as eq. 4, where I_{ex} and I_{mon} are respectively the emission fluorescence of the excimer and monomer excited forms, diminishes with an increase of the viscosity.

$$\frac{I_{ex}}{I_{mon}} = \frac{k_{f\,ex}}{k_{f\,mon}} \frac{[(Py...Py)^*]}{[Py]^*} = \frac{k_{f\,ex} k_d [Py]^*}{k_{f\,mon}(k_{-d} + k_{f\,ex})} \qquad \text{(eq. 4)}$$

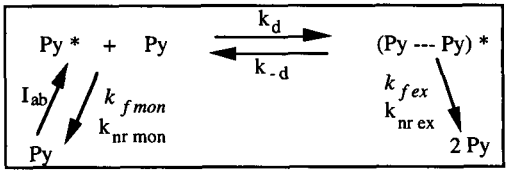

Fig. 2 : Kinetics scheme for fluorescence of pyrene (Ref. 7)

RESULTS AND DISCUSSION

Detection of the glass effect in bulk polymerization of MMA into PMMA

In discontinuous processes bulk polymerization is characterized by two effects which are respectively gel (Trommsdorff effect) and glass (vitrification effect), which are of great importance for the control of bulk polymerization operations (Fig. 3, Refs. 8, 9). The critical times of occurrence correspond to changes in the polymerization rate due to an increase in viscosity, a local overheating of the bulk and an hindered diffusion.

For the example of methyl methacrylate polymerization, the measure of the fluorescence emission efficiency of the cinnamylidene rotor (10^{-5} M ; λ_{ex} at 475 nm ; fluorescence emission measured at 565 nm with a 22.5° angle to the incident beam) with the polymerization time at a given temperature indicated a sharp increase at a specific time (Fig. 4). When the reaction time was converted into the monomer conversion, it was possible to correlate the ratio I_f/I_{f0} (where I_{f0} and I_f represent respectively the fluorescence intensity at time t = 0 and at time t) with the level of conversion (Fig. 5). The rise was observed for conversions near 80 % which corresponds to the vitrification range. At this stage of the polymerization, the viscosity of the medium is so large that it prevents intramolecular rotation of the excited state of the rotor with a subsequent decrease of the non radiative relaxation processes and then a simultaneous increase of the radiative deactivation with a higher fluorescence quantum yield (see eq. 1).

As a complementary information, use of intermolecular excimer formation for pyrene, which is sensitive to lateral diffusion, allows the detection of the gel effect. Indeed, for pyrene (10^{-3} M ; λ_{ex} at 322 nm ; fluorescence emission measured, with a 22.5° angle to the incident beam, at 393 and 474 nm for respectively the monomer (I_{mon}) and excimer (I_{ex}) forms), the variation of the ratio of the excimer intensity to the monomer intensity (I_{ex}/I_{mon}) was monitored with the polymerization time for the three temperatures considered (Fig. 6). The first period of the batch run, which was characterized by a high ratio remaining roughly constant, was followed by an abrupt decrease of the ratio which was then stabilized at low level. Here again, when the reaction time was converted into the monomer conversion, it was possible to correlate the ratio I_{ex}/I_{mon} with the level of conversion (Fig. 5). The decrease was observed for conversions roughly in the range 30 to 50 %, the starting of the decay in the excimer fluorescence corresponds to the beginning of the gel effect.

The critical times of both gel and glass effects, which were determined by using fluorescent sensors, allow the conversion and the molecular weights to be predicted for monomer conversions up to 90 % without adjustment of parameters as for usual models (Refs. 8, 10).

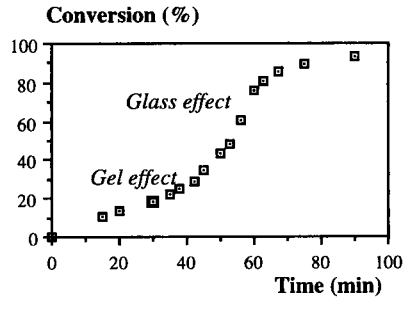

Fig. 3 : Typical representation of the conversion *versus* time for the bulk polymerization of MMA into PMMA, at 70 °C (see experimental part for the conditions).

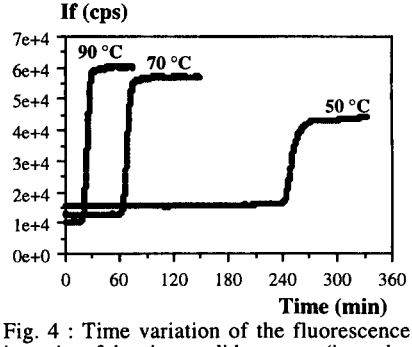

Fig. 4 : Time variation of the fluorescence intensity of the cinnamylidene rotor (in cycles per second) during the batch polymerization of MMA at three temperatures.

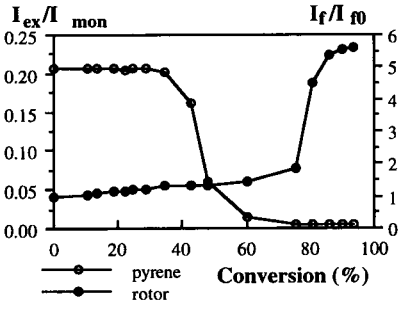

Fig. 5 : Variations of the ratio I_f/I_{f0} (right scale) for the cinnamylidene rotor and of the ratio I_{ex}/I_{mon} (left scale) for pyrene *versus* the rate of conversion for the polymerization of MMA at 70 °C (see text).

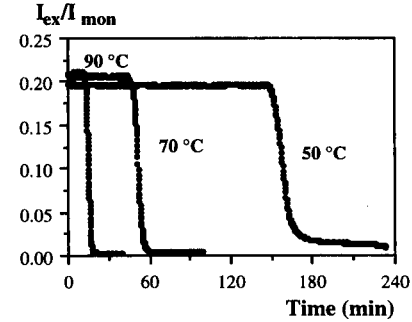

Fig. 6 : Time variation of the ratio for excimer fluorescence to monomer fluorescence for pyrene during the batch polymerization of MMA at three temperatures.

Detection of hydrophobic microdomains in amphiphilic polymers

Taking advantage of the dependence of the photophysical properties of the molecular cinnamylidene rotor on the polarity and the viscosity of the medium, the formation of hydrophobic microdomains for various water-soluble cationic amphiphilic polymers (*e.g.* polyvinylimidazolium bromides (Ref. 11) and polyvinylpyridinium bromides (Ref. 12)) was evidenced.

By increasing the polymer concentration (at 30 °C), both the fluorescence emission wavelength at its maximum, $\lambda_{f\,max}$, (Fig. 7) and the fluorescence efficiency (*i.e.* the relative fluorescence quantum yield, Φ_f/Φ_{f0}) (Fig. 9) were measured.

To get confidence in the results related to the rotor use, pyrene as a polarity probe was also used for polyvinylimidazolium bromides (Fig. 8). Note that pyrene was proved ineffective in the case of polyvinylpyridinium bromides because of fluorescence quenching due to the long alkyl chain quaternized pyridine.

Fig. 7 represents the variation of $\lambda_{f\,max}$ for the cinnamylidene rotor ($2.6\ 10^{-6}$ M ; λ_{ex} at 490 nm) as a function of the concentration for the methyl polymers PVIC1Br and P3VPC1Br, long alkyl chain polymers PVIC16Br and P3VPC16Br, their analogous surfactants HMIBr and HEPBr and a reference surfactant as CTABr.

As expected, no variation occurred for the methyl polymers. For conventional surfactants, an hypsochromic shift started at the critical micellar concentration (CMC) to reach, with the increasing concentration through a clear break, a final plateau value which represents the hydrophobic character of the local environment of the fluorescent probe. For long alkyl chain polymers, a similar profile was obtained with an earlier critical concentration (C_m, minimal concentration for the microdomains formation) and a rather progressive transition in comparison to the homologous surfactants. Moreover, the final plateau value for each polymer evidenced that their hydrophobic microdomains were less polar than the micelles formed with corresponding surfactants, indicating a restriction of the water penetration.

From each curve $\lambda_{f\,max}$ *vs* log C, it was possible to evaluate C_m or CMC values and also $\Delta\lambda_{f\,max}$ values which represent the overall hypsochromic shift related to the polarity lowering (Table 1).

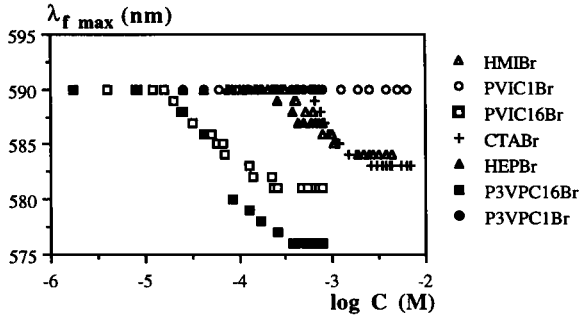

Fig. 7 : Variations of $\lambda_{f\,max}$ of the rotor (fluorescence emission at its maximum) with the concentration of polymers and surfactants (log. scale).

As indicated earlier, pyrene as a polarity probe was also used in the case of polyvinylimidazolium bromides and related compounds. Fig. 8 illustrates the dependence of the ratio I_1/I_3 for pyrene ($1.3\ 10^{-6}$ M ; excitation at 332 nm ; fluorescence emission recorded at 372 nm for the band 1 and at 383 nm for the band 3) as a function of the concentration, of either polymers PVIC1Br and PVIC16Br or surfactants HMIBr and CTABr.

As expected, no variation was observed for PVIC1Br which is quaternized by methyl groups. For the long chain alkyl polymer PVIC16Br, the ratio I_1/I_3 started to decrease at the C_m concentration in a rather broad range of concentrations. For the long chain surfactant HMIBr and the reference CTABr, a sharper transition appeared at a higher concentration (see Table 1). The lower value for the ratio I_1/I_3 at the final plateau for the polymer in comparison to the surfactant ones indicated a lower polarity microenvironment for the polymer, in agreement with the previous results related to the use of the molecular rotor.

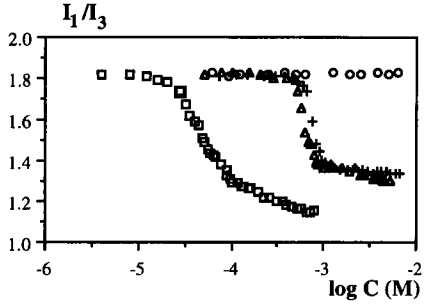

Fig. 8 : Variations of the ratio I_1/I_3 for pyrene with the concentration of polymers and surfactants (log. scale).

Owing to the dependence of the fluorescence quantum yield on viscosity (Ref. 1 and eq. 3), Fig. 9 shows the variation of the relative efficiency of the rotor Φ_f/Φ_{f0} (Φ_{f0} represents the fluorescence quantum yield in water) as a function of log C (polymer or surfactant concentration) for the same compounds as in Fig. 7 (rotor at $2.6\ 10^{-6}$ M ; λ_{ex} at 490 nm and fluorescence emission measured in the range 500-600 nm). As expected, no variation was observed for both methyl polymers PVIC1Br and P3VPC1Br. For surfactants and long chain polymers, due to the formation of either micelles or hydrophobic microdomains with higher local order an increase of the fluorescence emission efficiency was observed. Values of CMC, C_m and Φ_f/Φ_{f0} ratio are reported in Table 1.

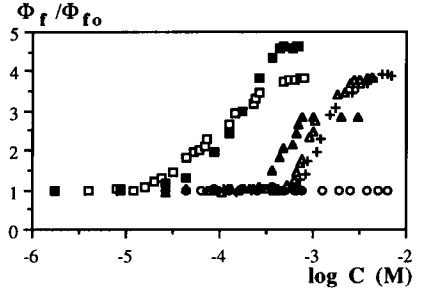

Fig. 9 : Variations of the fluorescence quantum yield ratio Φ_f/Φ_{f0} of the rotor with the concentration of polymers and surfactants (log. scale).

Table 1 : Data obtained from the use of the two fluorescent probes.

	Rotor					Pyrene		
	Polarity			*Cohesion*		*Polarity*		
Polymer or surfactant	$\lambda_{f\ max}$ (nm)	$\Delta\lambda_{f\ max}$ (nm)	CMC or C_m (mol/L)	Φ_f/Φ_{f0}	CMC or C_m (mol/L)	I_1/I_3	$\Delta(I_1/I_3)$	CMC or C_m (mol/L)
PVIC16Br	581	9	$1.6\ 10^{-5}$	3.8	$1.65\ 10^{-5}$	1.15	0.66	$1.7\ 10^{-5}$
HMIBr	584	6	$4\ 10^{-4}$	3.8	$4.3\ 10^{-4}$	1.33	0.51	$4.5\ 10^{-4}$
P3VPC16Br	576	14	$2.3\ 10^{-5}$	4.6	$2.5\ 10^{-5}$	No possible values due to		
HEPBr	587	3	$3.9\ 10^{-4}$	2.8	$3\ 10^{-4}$	quenching phenomena		
CTABr	583	7	$6.3\ 10^{-4}$	3.9	$6.3\ 10^{-4}$	1.34	0.47	$5\ 10^{-4}$

A good agreement was observed for the CMC and C_m values in respect to the different fluorescence probes (rotor or pyrene) and the environmental parameter (polarity or viscosity). A deeper discussion could be find elsewhere (Refs. 3, 12).

Incorporation in polymer beads

By using emulsion polymerization, incorporation of fluorescent molecular rotors was achieved in PMMA beads. The resulting beads were analysed for their fluorescence behaviour in several host media (solvents, silicone oils, polymers, etc.) (Ref. 13) and their potential applications are under investigation.

EXPERIMENTAL PART

Materials

The fluorescent rotor was synthesized by a Knoevenagel's reaction between (4-dimethylamino)-cinnamaldehyde and malononitrile [m.p. = 147 °C ; literature 146-148 °C (Ref. 14)]. Pyrene was purchased from the Community Bureau Reference (n° 177).

MMA from Fluka was first dried on calcium hydride, then filtered before distillation by the cold wall technique and stored after distillation at - 20 °C in a stopped vessel previously purged with argon. AIBN (α,α'-azoisobutyronitrile) was a Merck product, recrystallized from methanol. The synthesis of the cationic polymers (P3VPC1Br, P3VPC16Br, PVIC1Br, PVIC16Br) and cationic surfactants (HMIBr and HEPBr) has been described elsewhere (Refs. 3, 11). Commercial CTABr from Fluka was purified according to a classical method (Ref. 12).

Absorption and fluorescence spectra

Absorption spectra were recorded on a Perkin Elmer (Lambda 2) UV-visible spectrophotometer. Fluorescence emission spectra were recorded on a SPEX Fluorolog-2 spectrofluorimeter equipped with a thermostated cell compartment.

Polymerization of MMA

Discontinuous polymerization was carried out under nitrogen flow in a 3 cm^3 Pyrex tube, 10 mm in diameter and provided with a double jacket and ground stoppers. The tube was placed in the thermostated cell compartment of the spectrofluorimeter at the chosen temperature (temperature control within 0.5 °C). Radical polymerization of MMA was initiated by AIBN (0.5 wt.-%) and run in the presence of the fluorescent probe. The conversion of monomer was determined by the usual gravimetric technique.

Solutions of cationic polymers and surfactants

Solutions were prepared by dissolving the polymer or the surfactant in an aqueous mixture (ethanol/1-propanol/water, 1/3/96 vol.-%). The probe (stock solution in ethanol) was added in the solutions already formed (less than 0.35 vol.-% added by this introduction).

Polymerization in emulsion to include fluorescent rotors in polymer beads

The aqueous reaction mixture contained sodium dodecyl sulfate (Sigma) at 0.5 wt.-% as the surfactant, MMA (Fluka) at 1.6 M, 4,4'-azobis(4-cyanovaleric acid) (Aldrich) at 1 wt.-% as the initiator and the rotor (for exemple 1-cyano-1-ethoxycarbonyl-4-(4'-dimethylaminophenyl)-1,3-butadiene) at 7 10^{-5} M). The reaction was run under stirring at 60 °C.

CONCLUSION

Fluorescence spectroscopy using a cinnamylidene molecular rotor as a viscosity probe was proved to be a complementary method to the one using pyrene for the monitoring of the bulk polymerization of MMA to PMMA. In the case of amphiphilic cationic polymers, informations from the use of both rotor and pyrene are in good agreement regarding the polarity. Moreover, the rotor (in addition to the fact that it is less sensitive to quenching phenomena than pyrene) leads to information on the local cohesion, which could be corroborated to structural arrangements of the assemblies (Ref. 15, in this volume). Finally, inclusion of the molecular fluorescent rotors in polymers beads will be of interest for further fluorescence tracing studies.

REFERENCES

(1) R.O. Loutfy, B.A. Arnold, *J. Phys. Chem.* **86**, 4205 (1982)

(2) W. Rettig, *Top. Curr. Chem.* **169**, 253 (1994)

(3) A. Benjelloun, A. Brembilla, P. Lochon, M. Adibnejad, M.L. Viriot, M.C. Carré, *Polymer* **37**, 879 (1996)

(4) K.Y. Law, *Chem. Phys. Lett.* **75**, 545 (1980)

(5) A.K. Doolittle, *J. Appl. Phys.* **23**, 236 (1952)

(6) D.C. Dong, M.A. Winnik, *Can. J. Chem.* **62**, 2560 (1984)

(7) J.B. Birks, *Photophysics of aromatic molecules*, Wiley-Interscience, New York 1970

(8) K. Mulyono, C. Schrauwen, F. Pla, M. Adibnejad, M.L. Viriot, J.C. André, *Récents Progrès en Génie des Procédés*, Lavoisier, Paris **9**, 31 (1995)

(9) S.T. Balke, A.E. Hamielec, *J. Appl. Polym. Sci.* **17**, 905 (1973)

(10) J. Villermaux, L. Blavier, *Chem. Eng. Sci.* **39**, 87 (1984)

(11) C. Damas, A. Brembilla, P. Lochon, F. Baros, M.L. Viriot, *Eur. Polym. J.* **30**, 1215 (1994)

(12) C. Damas, M. Adibnejad, A. Benjelloun, A. Brembilla, M.C. Carré, M.L. Viriot, P. Lochon, *Colloid Polym. Sci.* **275**, 364 (1997)

(13) F. Thauvin, M.C. Carré, M.L. Viriot, J.C. André, *Proceedings of the 4ème Congrès National de la Société Française de Chimie*, Strasbourg, 17-20 september (1991)

(14) M. Matsuoka, M. Takao, T. Kitao, T. Fujiwara, K. Nakatsu, *Mol. Cryst., Liq. Cryst.* **182A**, 71 (1990)

(15) A. Benjelloun, C. Dorion, A. Brembilla, M.L. Viriot, M. Adrian, *This Volume* (1997)